Cent. Eur. J. Geosci. • 5(2) • 2013 • 208-222
DOI: 10.2478/s13533-012-0124-9

VERSITA

Central European Journal of **Geosciences**

Combining SPOT 5 imagery with plotwise and standwise forest data to estimate volume and biomass in mountainous coniferous site

Research Article

Petar K. Dimitrov[1]* Eugenia K. Roumenina[1]

1 Space Research and Technology Institute Bulgarian Academy of Sciences 1113 Sofia, Acad. G. Bonchev St, bl. 1, Bulgaria

Received 3 January 2013; accepted 25 March 2013

Abstract: In this study, regression-based prediction of volume and aboveground biomass (AGB) of coniferous forests in a mountain test site was conducted. Two datasets - one with applied topographic correction and one without applied topographic correction - consisting of four spectral bands and six vegetation indices were generated from SPOT 5 multispectral image. The relationships between these data and ground data from field plots and national forest inventory polygons were examined. Strongest correlations of volume and AGB were observed with the near infrared band, regardless of the topographic correction. The maximal correlation coefficients when using plotwise data were -0.83 and -0.84 for the volume and AGB, respectively. The maximal correlation with standwise data was -0.63 for both parameters. The SCS+C topographic correction did not significantly affect the correlations between spectral data and forest parameters, but visually removed much of the topographically induced shading. Simple linear regression models resulted in relative RMSE of 32-33% using the plotwise data, and 43-45% using the standwise data. The importance of the source and the methodology used to obtain ground data for the successful modelling was pointed out.

Keywords: regression • multispectral imagery • coniferous forest • forest inventory • Rila Mountain

1. Introduction

Forests in the south of Europe are predominantly concentrated in isolated mountain areas surrounded by greatly transformed agricultural and urban environments. The Rila-Rhodopes massif in particular gives refuge to a large forest patch, which has substantial significance both for the forestry industry and the maintenance of the ecological stability in the region. Coniferous boreal species dominate here because of the altitude, and some rare endemic forest communities are also present. The management and protection of these forests requires quantifying and spatially presenting different forest parameters. Timber volume, for example, is traditionally used to characterize growing stock; while biomass assessment is increasingly discussed in the context of the full utilisation of all tree components [1]. Forest biomass data is also needed in regional and global carbon stock studies and climate modelling. However, acquiring such data is a major issue because of the complex topography in the mountainous regions. Making a field inventory is labour consuming and expensive, and

*E-mail: petarkirilov@mail.bg

in Bulgaria data is being updated at only every ten years.

Estimation of volume and biomass of coniferous forests using remote sensing data has a relatively long history. Different methods have been proposed, with regression analysis still being among the most commonly used one. In this empirical method, a forest attribute is related to surface reflectance or spectral vegetation indices (SVIs) derived from reflectance. The method is characterized by its simplicity and well established theoretical (statistical) basis. The weaknesses of its application are also well understood [2, 3]. However, some of the problems with regression are present in other commonly used methods like neural networks and kNN [4, 5].

To derive the regression relationship, one should consider the scale. It is dependant on the type of forest inventory data, which are typically available at plot or stand level. Both types of data have been used [6–10] with no commonly accepted preference. The effect of scale on the strength of relationships is manifested through the susceptibility to geometric errors in data and to the stand border conditions, which have been found to be a major factor in forest attributes estimation [8]. Muukkonen and Heiskanen [4] discussed that the use of standwise data may solve the problems arising from the errors in image registration and location of sample plots.

The fragmented nature and the relatively small size of the stands of many mountain forests suggest that satellite images with an appropriately fine spatial resolution should be used for volume and biomass estimation. The High Resolution Geometric (HRG) sensor onboard the Satellite Pour l'Observation de la Terre (SPOT) 5 satellite provides multispectral images with 10 m pixel size, which seems to be perfectly suited for forest mapping under the described conditions. Since the pixel size is slightly larger than the typical crown size of conifers, SPOT 5 provides the finest possible resolution without resolving individual trees. Very high resolution satellite and aerial images with pixel size as small as 1.0 m are increasingly utilized for forest parameter estimation. In many studies using such data, however, information is aggregated to the smaller scale, and as with lower resolution sensors, the reliance is on the relative proportion of shade cast by the trees [7, 11].

Widely acknowledged problem hindering automated information extraction from satellite images in mountainous areas is the difference in illumination of slopes with different steepness and azimuth angles. For the same cover type, the satellite sensor will register higher radiance when observing on slope facing the Sun and lower radiance when observing on slope tilted in the opposite direction. These differences may mask the real reflection characteristics of objects and should be removed or diminished. The application of topographic correction is believed to reduce the influence of topographic effects in favour of the intrinsic reflection properties of objects [12], thus providing for more accurate determination of the biophysical properties of the surface. It has been shown that a non-Lambertian topographic correction model can improve the accuracy of land cover classification [13] and constitute an important step in obtaining physically reliable and homogeneous time series [14]. Comparing raw data with topographically corrected data, Dorren *et al.* [15] show that the classification errors in the case when uncorrected images were used are more concentrated in faintly illuminated pixels and that topographic correction improves the accuracy of Landsat TM-based forest stand type maps in steep mountainous terrain. Using the statistic-empirical, Minnaert and C-correction approaches, Meyer *et al.* [12] also found an improvement in forest classification. The correction of topographic effects is most often discussed and assessed with respect to image classification procedures. In forest environment, these effects can be expected to affect not only the possibility for separating different forest types, but also the regression-based estimation of forest parameters. Moreover, in this type of analysis, pixel brightness is most often expected to carry the information of interest.

The general objective of this study is to examine the possibility for estimation of tree volume and aboveground biomass (AGB) of coniferous forests in high relief using multispectral SPOT 5 imagery combined with ground truth data at different scale. For the purpose, the prediction capabilities of the SPOT 5 spectral bands and six spectral vegetation indices from topographically corrected and from uncorrected image are assessed. The results from the use of plotwise and standwise ground data are compared and the differences and advantages of each type of data are discussed.

2. Study area

A region of ~200 km^2 located on the northern slope of the Rila Mountain (SW Bulgaria) was selected for the study (Figure 1). Seventy percent of the territory is covered by coniferous forests, which spread from 1000 m a.s.l. to the tree line at 1800-2100 m a.s.l. They are composed by Scots pine (*Pinus sylvestris* L.), Norway spruce (*Picea abies* (L.) Karst.), silver fir (*Abies alba* Mill.), and Macedonian pine (*Pinus peuce* Griseb.). These species form pure and mixed stands with even and uneven age structures [16]. Hazel and juniper shrubs, and grass are present in the understory where stands are more open. Most stands are with high canopy cover (75-85%). The

oldest stands are up to 120 years old. Part of the forests in the study area is managed for timber production and other part falling in the "Rila" National park is protected.

3. Material and methods

The methodology of the study consists of several steps. Firstly, ground reference data for volume and AGB was collected from two separate sources - sample plot measurements made for this study and stand level national forest inventory (NFI) data. Secondly, a SPOT 5 image was geometrically corrected, calibrated to at-sensor radiances and used to calculate several SVIs. Additionally, using DEM, a topographically corrected image was prepared from which SVIs were also calculated. Thirdly, the values of the four bands and the SVIs from the two images were extracted for each field plot and NFI stand and correlated with the volume and AGB data to select the most suitable satellite variable to be used for modelling. Finally, using the plot and stand data separately, two sets of regression models for volume and AGB were developed and then validated and compared. These steps are presented in more details in Figure 2 and in the next paragraphs.

3.1. Ground data

3.1.1. Plot measurements

Thirty-two temporary plots were established in the study area. The sampled stands were selected using information from available forest inventory maps and satellite images with the intention to represent a wide range of age classes and structural diversities. Depending on the density of trees, square plots of 25 m^2 to 900 m^2 were used. On the field, the location of plots was determined according to the following criteria: to be in homogeneous part of the stand, and to be at least 20-30 m apart from stand borders (the second condition was violated for the youngest stands only due to the difficult access). Diameter at breast height (DBH), height and species was recorded for every tree with DBH>10 cm in forests older than ~20 years, and with DBH>2 cm otherwise. In some plots, part or all trees were not measured for height, but their height was estimated based on the DBH using height curves calculated from the available measurements from the plots. The geographic coordinates at the centre of each plot were determined by averaging three 15-minutes GPS measurements with differential corrections applied during post processing. The volume (of stem) of each tree, V_t (m^3), was calculated using the equation provided in Beruchashvili and Zhuchkova [17]:

$$V_t = 0.534 \cdot H \cdot D^2 \cdot q_2, \quad (1)$$

where H is the tree height (m), D is the DBH (m), and q_2 is the ratio of the diameter at half tree height to the DBH. The values of q_2 used were: 0.70 for spruce and fir, and 0.65 for pines [18]. The volume of all trees was summed by species and expressed to a hectare. The dry AGB of each species ($t\,ha^{-1}$) was determined by multiplying the volume ($m^3\,ha^{-1}$) by the timber density ($t\,m^{-3}$) and adding the biomass of branches and foliage. The average values for timber density and percentage of branches' and foliage' biomass from the stem biomass by species, were taken from Beruchashvili and Zhuchkova [17]. The volume measured in the plots varied from 47 $m^3\,ha^{-1}$ to 985 $m^3\,ha^{-1}$. The AGB was in the interval 21-462 $t\,ha^{-1}$. The mean values can be seen in Table 7. Plots with AGB less than 100 $t\,ha^{-1}$ were found as a rule in pure Scots pine forests with even aged structure and age of up to 20-30 years. Some of these stands are plantations. The composition and structure of the stands where higher AGB was measured were highly variable -from pure Scots pine and Norway spruce stands to mixed stands and from one-storeyed and relatively open stands to multilayered dense stands (Figure 3).

3.1.2. National forest inventory data

A NFI dataset, which covers part of the study area, was available. The NFI data are presented at stand (sub-compartment) level and include several parameters from which mean diameter, mean height and volume by forest layers and tree species in the layers were used. A polygonal layer with the borders of the sub-compartments was created in GIS by digitizing them from map of forest sites in scale 1:25000. The dataset was filtered by stand size, and 795 stands with area over one hectare remained to be used in the further analysis. The mean area of the stands was 5.9 ha. The AGB of each stand was calculated using species-specific coefficients for conversion from stand volume to biomass of different parts - stem, branches and foliage [19]. For the stem, single coefficient was used, while the coefficients for branches and foliage should be calculated for each tree layer and/or species separately based on the mean diameter and height [19]. The full AGB of a stand was derived by the sum of the biomasses calculated for each tree layer and/or species within the layer. Coefficients for Macedonian pine and silver fir are not provided in Zamolodchikov *et al.* [19] and for these species the coefficients for Scots pine and Norway spruce were used instead. Since deciduous tree species are very rare in the studied stands, their

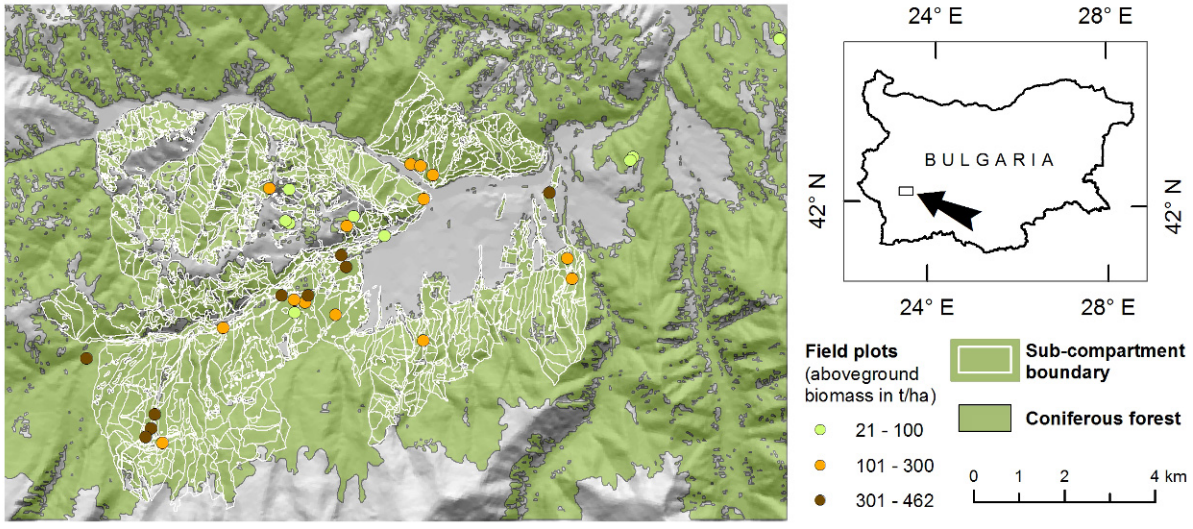

Figure 1. Map of the study area showing the coverage of the national forest inventory polygons from which data was used and the location of the field plots. The extent of coniferous forests was mapped by unsupervised classification of the SPOT 5 image.

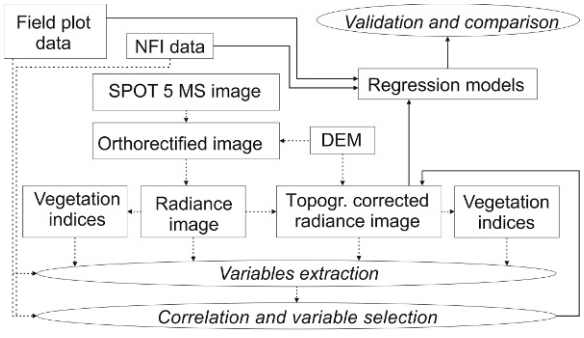

Figure 2. Flow chart of the data processing and analysis steps in the study. The steps shown with dashed lines were first implemented followed by these shown with solid lines.

biomass was ignored. The biomass of understorey was also not taken into account. Stand volume and AGB data was randomly split into training (70%) and validation dataset (30%).

3.2. Image pre-processing

A level 1A scene from SPOT 5 acquired on 14 July 2008 was used in this study. The panchromatic image was first orthorectified, using 32 GPS ground control points (GCPs) and an ASTER GDEM v.2 digital elevation model [20] yielding a 0.8 pixels RMSE (accuracy assessment based on 14 independent check points). The panchromatic image was then used as a base image to orthorectify the multispectral image with RMSE of 0.5 pixels (accuracy assessed by 9 independent check points). Only the four spectral bands (XS1:0.49-0.60 μm; XS2:0.61-0.68 μm; XS3:0.78-0.89 μm; SWIR:1.54-1.75 μm) were used in the further analysis. The digital numbers were converted to radiances, L, ($W\,m^{-2}\,sr^{-1}\,\mu m^{-1}$) using the coefficients provided with the image metadata [21]. Since our major goal was to assess the relative performance of plotwise and standwise ground data, as well as the effect of topographic correction on a single image, the atmospheric effects and their correction was not dealt with in this study.

From the radiance image a topographically corrected image was also prepared. Different models have been proposed for correction of topographic effects on satellite imagery (see [23] for review), the simplest one representing a modification of the cosine correction involving the solar zenith angle ([24] cited by Kane *et al.*, [23]). This cosine correction, however, only models the direct part of the irradiance, while the weakly illuminated regions may get a considerable amount of diffuse irradiance as well [12]. Overcorrection of the weakly illuminated pixels is characteristic for the cosine corrected images. This method proved to be inappropriate for sloped terrains [12, 24]. Methods like the Minnaert and C-correction can greatly diminish overcorrection by

Figure 3. Typical forest stands in the study area: (a) pure Scots pine, even-aged stand - 220 t ha^{-1} AGB; (b) pure Norway spruce, even-aged stand - 257 t ha^{-1} AGB; (c) mature Scots pine stand with sparse lower tree layer composed of Norway spruce - 420 t ha^{-1} AGB.

incorporating empirically derived constants in the cosine model. Gu and Gillespie [25] proposed a new approach intended specifically for application on forest images – the Sun-Canopy-Censor (SCS) model – which normalize the mutual shadowing of trees.

In this study, the SCS+C model [26] was used, which is a modification of the model proposed by Gu and Gillespie [25]. In this model, the parameter C is added similarly to the c-corection method. The topographically corrected radiance (TC radiance), L_0, was calculated using the following equations [26]:

$$L_0 = L\frac{\cos\alpha\cos\theta + C}{\cos i + C} \tag{2}$$

$$\cos i = \cos\theta\cos\alpha + \sin\theta\sin\alpha\cos(\varphi) \tag{3}$$

where L is the radiance of the uncorrected pixel, α is the slope of the pixel, θ is the solar zenith angle, i is the incidence angle relative to the normal of the pixel, φ is the difference between the pixel exposition and the solar azimuth angles, and C is empirical constant. The constant C is equal to a/b, where a and b are coefficients in the regression equation $L = a + b \cdot \cos i$. Adding of C is used to better characterize diffuse sky irradiance (downwelling spectral irradiance at the surface due to scattered solar flux in the atmosphere) and thus to reduce the overcorrection of faintly illuminated pixels [26]. The constant C was calculated for the coniferous forests only. For the purpose, a random sample of 15000 pixels representing coniferous forests was used, and for each pixel, the radiance in the four bands and $\cos i$ were extracted. Based on these data, the regression coefficients, and from them, C was found for each spectral band. To apply the correction, ASTER GDEM v2 was used after resampling from the original resolution (30 m) to the spatial resolution of the SPOT 5 image (10 m).

Six SVIs were calculated both from the original radiance spectral data and the topographically corrected data (TC radiance). They are presented in Table 1 and include common indices based on the near infrared (NIR) and the short wave infrared (SWIR) spectral bands used in most forest studies.

3.3. Regression analysis and validation

The satellite variables - bands' radiances and vegetation indices - were extracted from the images to explain the volume and AGB. At plot level, the average of the four closest pixels to the plot's centre was used. The average of all pixels within a stand was extracted using the GIS layer with the stand borders. The pixels coinciding with the borders were excluded from the calculation because they receive signal from two or more adjacent stands [8]. Simple linear regression, with the NIR band as independent variable, was used to model the volume and AGB. To deal with heteroscedasticity problems and non-linearity, base-10 logarithm transformation was considered for y, x or both variables. The increase in R^2 was used as a measure when deciding whether a transformation of variables was needed. It was found that in all cases, the dependent variable, y, should be transformed. In this way, the linear regression equation will give the volume and AGB in logarithms. When the coefficients of this equation, b_0 and b_1, are found, y can be calculated in the original units using equation (4); or using equation (5) if the independent variable, x, was also transformed [33]:

$$y = 10^{b_0} \cdot 10^{b_1 \cdot x} \cdot 10^{\varepsilon} \tag{4}$$

$$y = 10^{b_0} \cdot x^{b_1} \cdot 10^{\varepsilon} \tag{5}$$

Table 1. Vegetation indices used in the study.

Index	Formula	Reference
Normalised Difference Vegetation Index (NDVI)	NIR – Red / NIR + Red	[27]
Corrected NDVI (NDVIc)	NDVI · (1 – (SWIR – SWIRmin) / (SWIRmax – SWIRmin))	[28, 29]
Simple Ratio (SR)	NIR / Red	
Reduced Simple Ratio (RSR)	SR ·(1 – (SWIR – SWIRmin) / (SWIRmax – SWIRmin))	[30]
Normalised Difference Infrared Index (NDII)	NIR – SWIR / NIR + SWIR	[31]
Structural Index (SI)	NIR / SWIR	[32]

In the back-transformation using (4) and (5), the error term, ε, is included as suggested by Newman [33] to correct statistical bias. The procedure outlined in Newman [32] was used:

$$10^{\varepsilon} = 10^{MSE/2}, \quad MSE = \sum_{i=1}^{n} \frac{e_i^2}{n-2} \tag{6}$$

where MSE is the mean square of the error from the regression, e_i is the residual for observation i, and n is the number of observations.

After applying back-transformation, the modelled values of volume and AGB, $\hat{y}_i$ were compared with the measured values y_i, and two accuracy statistics - the root mean square error ($RMSE$) and the $Bias$ - were calculated [4]:

$$RMSE = \sqrt{\frac{1}{n}\sum_{i=1}^{n}(y_i - \hat{y}_i)^2} \tag{7}$$

$$Bias = \frac{1}{n}\sum_{i=1}^{n}(y_i - \hat{y}_i) \tag{8}$$

Their relative counterparts, $RMSE_r$ and $Bias_r$ were calculated as a percent of the mean measured value of the forest parameter. The significance of $Bias$ was tested using the t-statistic ($df = n - 1$) := $Bias/(SD/\sqrt{n})$, where SD is the standard deviation of the residuals [4]. To calculate the accuracy statistics for the models at stand level, the validation stands were used. For the models at plot level, leave-one-out cross validation was used.

4. Results

4.1. Correlations

All spectral bands of SPOT 5 and the SVIs, except NDVIc, were statistically significantly correlated with the volume and AGB in the plots (Table 2). For both parameters, the strongest correlations were with the near infrared (XS3) band of SPOT 5 ($r = -0.83$ for volume and $r = -0.84$ for AGB; $p < 0.001$), followed by the correlations with NDVI and SR. From the spectral bands, the correlations with the red (XS2) band were consistently lowest. The vegetation indices which use the SWIR band showed significantly lower correlations relative to the SWIR band itself.

The volume and AGB of the stands were also statistically significantly correlated with the four bands, and NDVI and SR, but were not correlated with any of the indices using the SWIR band (Table 3). As for the plots, the maximal correlations for both forest parameters were obtained with the NIR band ($r = -0.63$; $p < 0.001$), followed by the NDVI, SR, and the green (XS1), SWIR, and red bands. Because the data for volume and AGB from the stands, as well as the corresponding satellite variables extracted from the stands, were not normally distributed, the Pearson product-moment correlation coefficient (r) used here may be misleading. Therefore, the nonparametric correlation coefficient of Spearman (r_s) was also calculated (Table 4). It displayed the same pattern in the correlations as the Pearson's coefficient.

The correlations reported above are for the original uncorrected image. Very close correlation coefficients were obtained when using the topographically corrected image. However, in most cases, the correlation coefficients with the original data were slightly higher, especially for the stands. The test for equality of correlation (Table 5) showed that these differences were not statistically significant. The correlations of both forest parameters with the NIR band of SPOT 5 were significantly different at plot and stand level ($Z = -2.600$; $p = 0.009$ and $Z = -2.598$; $p = 0.009$ for volume and AGB respectively; results for the TC Radiance data).

4.2. Regression models

Since the two forest parameters showed highest correlation with the near infrared band (XS3) of SPOT 5, this band was used as predictor in the regression analysis. The TC radiance data was used. The regression models developed using both data from the plots and the stands, as well as their accuracy statistics, are presented on Table 6. At plot level, the NIR band explained 77% of

Table 2. Correlation coefficients between the volume and AGB from the plots and the spectral bands and indices from SPOT 5.

	XS1	XS2	XS3	SWIR	NDVI	SR	NDII	SI	NDVIc	RSR
	Pearson product-moment correlation coefficient (r)									
	Volume									
Radiance	-0.69***	-0.57**	-0.83***	-0.63***	-0.79***	-0.77***	-0.47**	-0.50**	-0.34	-0.41*
TC Radiance	-0.71***	-0.57**	-0.82***	-0.62***	-0.77***	-0.75***	-0.46**	-0.49**	-0.34	-0.41*
	AGB									
Radiance	-0.72***	-0.60***	-0.84***	-0.66***	-0.78***	-0.77***	-0.44*	-0.47**	-0.32	-0.39*
TC Radiance	-0.73***	-0.59***	-0.82***	-0.64***	-0.76***	-0.75***	-0.44*	-0.47**	-0.32	-0.39*

*, **, and *** indicate significance at 0.05, 0.01 and 0.001 level, respectively

Table 3. Correlation coefficients between the volume and AGB from the training stands and the spectral bands and indices from SPOT 5.

	XS1	XS2	XS3	SWIR	NDVI	SR	NDII	SI	NDVIc	RSR
	Pearson product-moment correlation coefficient (r)									
	Volume									
Radiance	-0.53***	-0.45***	-0.63***	-0.50***	-0.57***	-0.56***	-0.07	-0.13**	0.03	-0.04
TC Radiance	-0.48***	-0.40***	-0.58***	-0.46***	-0.49***	-0.50***	-0.04	-0.10*	0.04	-0.03
	AGB									
Radiance	-0.55***	-0.47***	-0.63***	-0.52***	-0.57***	-0.56***	-0.04	-0.10*	0.05	-0.02
TC Radiance	-0.49***	-0.41***	-0.59***	-0.47***	-0.48***	-0.49***	-0.01	-0.07	0.07	-0.01

*, **, and *** indicate significance at 0.05, 0.01 and 0.001 level respectively

the variations in the volume and 76% of the variations in the AGB. The modelling of the volume yielded a RMSE of 152.4 $m^3\,ha^{-1}$, while the error of the AGB model was 70.2 $t\,ha^{-1}$. The $RMSE_r$ was quite near for the two forest parameters (Table 6). The biases of the estimates of the two models were not significant. Moreover, the residuals were normally distributed as indicated by the Shapiro-Wilks test for normality ($W = 0.968$; $p = 0.435$ and $W = 0.967$; $p = 0.423$ for the volume and AGB, respectively). The scatter plots (not shown) of standardized residuals versus standardized estimates showed that the residuals have constant variance and do not follow any pattern. The plots in Figure 4a and Figure 4b show generally good agreement of the plot-measured volume and AGB, on the one hand, and their modelled values, on the other hand.

The R^2 values were lower for the models based on the stand-averaged NFI data. The NIR band explained only 42-43% of the variations in the volume and AGB (Table 6). In accordance with this, the standard errors of estimate (SEE) and the RMSEr were higher than those of the models utilizing plot level data. However, the RMSE was the same or even lower for the stand-level models. The relative performance of the stand and plot models was inconsistent according to the SEE and RMSE statistics. This could be due to the fact that the RMSE was calculated by cross-validation procedures and the relative performance of the models may have changed in the validation runs. As with the first two models, the biases were not significant, but the Shapiro-Wilks test indicated that residuals were not normally distributed ($W = 0.967$ and $W = 0.965$ for the volume and AGB respectively; $p < 0.001$). Relatively poor agreement was observed between ground data and the modelled values of stands' volume and AGB (Figure 4c and Figure 4d). For these two models, some underestimation of the high values and overestimation of the low values was obvious.

In Figure 5, fragments from maps of volume created using the NFI dataset and the two regression models are compared. For better comparison, the volume was represented in six classes. The map created using the regression model generated from stand data (Figure 5a) was relatively accurate in reviewing the spatial distribution of volume as presented in the NFI data (Figure 5c). There were, however, differences of one or more classes in some places between the two maps. Large overestimation was observed for the regression map based on plot data (Figure 5b) as compared with the ground NFI data. In fact, using this regression model, the volume was estimated to be over 500 $m^3\,ha^{-1}$ for most of the territory. This result was confirmed also by the comparison of the area covered by each volume class (Figure 6a). The area estimates were quite close for the NFI data and the SPOT 5 regression map based on this data (i.e. the stand model), especially for the interval from 100 to 500 $m^3\,ha^{-1}$. The inaccuracies in the satellite map were larger for the marginal classes - the class from 1 to 100 $m^3\,ha^{-1}$ featured area twice as small, while the class over 500 $m^3\,ha^{-1}$ featured area twice as large than the

Table 4. Spearman's correlation coefficients between the volume and AGB from the training stands and the spectral bands and indices from SPOT 5.

	XS1	XS2	XS3	SWIR	NDVI	SR	NDII	SI	NDVIc	RSR
	Spearman's rank correlation coefficient (rs)									
	Volume									
Radiance	-0.55	-0.49	-0.65	-0.50	-0.55	-0.55	-0.14	-0.15	-0.07	-0.12
TC Radiance	-0.50	-0.44	-0.63	-0.47	-0.47	-0.47	-0.11	-0.12	-0.04	-0.10
	AGB									
Radiance	-0.57	-0.51	-0.67	-0.54	-0.56	-0.56	-0.10	-0.11	-0.05	-0.10
TC Radiance	-0.51	-0.45	-0.63	-0.50	-0.47	-0.47	-0.07	-0.08	-0.01	-0.07

Table 5. Results from the equality test of correlation coefficients obtained using radiance and terrain corrected radiance data ($H_0 : \rho_1 = \rho_2$). The test statistic Z and its p-values are presented. None of the compared correlations differed significantly (all p-values are over 0.05).

	Radiance vs terain corrected radiance								
	XS1	XS2	XS3	SWIR	NDVI	SR	NDII	SI	RSR
	Z-statistic (p-value)								
Plots:									
Volume	0.113	-0.029	-0.097	-0.122	-0.147	-0.162	-0.029	-0.035	-0.001
	(0.910)	(0.977)	(0.923)	(0.903)	(0.883)	(0.871)	(0.977)	(0.972)	(0.999)
AGB	0.064	-0.059	-0.170	-0.162	-0.192	-0.201	-0.032	-0.039	-0.006
	(0.949)	(0.953)	(0.865)	(0.871)	(0.848)	(0.840)	(0.974)	(0.969)	(0.995)
Stands:									
Volume	-1.188	-1.066	-1.142	-0.963	-1.798	-1.506	-	-	-
	(0.235)	(0.287)	(0.253)	(0.336)	(0.072)	(0.132)			
AGB	-1.294	-1.139	-1.280	-1.016	-1.932	-1.620	-	-	-
	(0.196)	(0.255)	(0.200)	(0.309)	(0.053)	(0.105)			

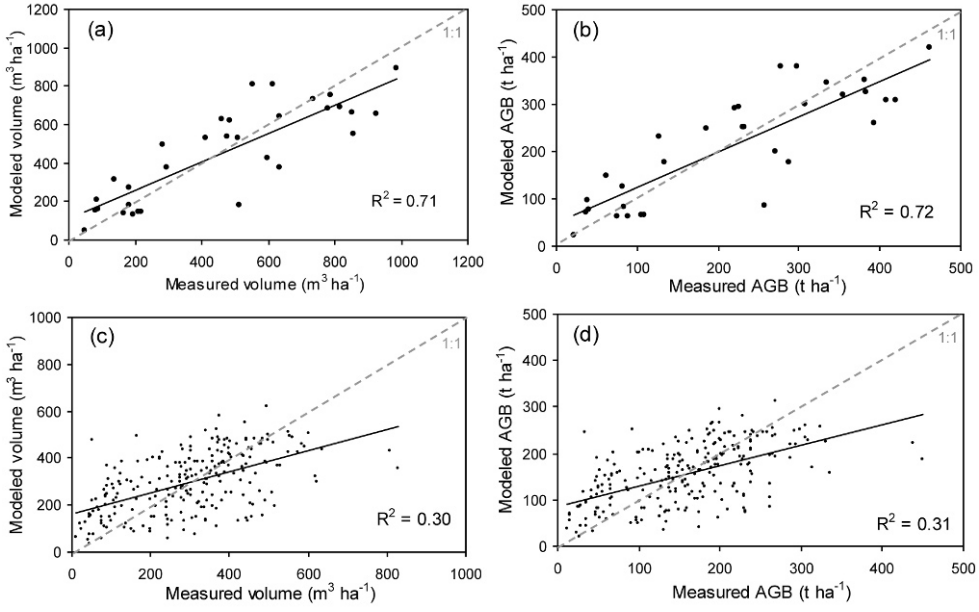

Figure 4. Results from the validation of the regression models for prediction of volume and aboveground biomass: (a) and (b) - models based on plot data; (c) and (d) models based on stand data.

Table 6. Regression models for volume and AGB developed by plot and stand data.

Nº		Regression parameters			Validation						
		$\log Y = (b_0 + b_1 X_1)^*$		R^2	SEE	MSE	*RMSE*	$RMSE_r$ (%)	*Bias*	$Bias_r$ (%)	*p*-value
		b_0	$b_1 X_1$								
	Plots:										
1	Volume *	4.046	-0.029 (NIR)	0.77	0.177	0.031	152.4	33.0	9.9	2.1	0.719
2	AGB *	3.726	-0.029 (NIR)	0.76	0.183	0.033	70.2	32.4	4.6	2.1	0.717
	Stands:										
3	Volume *	8.799	-3.837 (log NIR)	0.42	0.280	0.078	136.5	45.4	2.2	0.7	0.809
4	AGB *	8.128	-3.596 (log NIR)	0.43	0.260	0.067	69.0	43.5	1.9	1.2	0.672

* The dependant variable is base-ten log-transformed;
SEE–standard error of estimate (in logarithms);
MSE–mean square of the error (residuals) from the regression.

NFI map. However, these differences are small compared with the discrepancy between the areas from the NFI map and the SPOT 5 regression map based on plot data (Figure 6a). The mean volume by age class for the three maps was also compared (Figure 6b). The Wilcoxon paired signed-rank test ($Z = -1.352$; $p = 0.176$) did not show significant difference between the estimates obtained from the stand model and the NFI data. The mean volume estimates obtained from the plot model were consistently higher then those from the NFI data.

5. Discussion

5.1. Correlations

The relationship of volume and AGB with the SPOT 5 NIR band (Figure 7) observed in this study was similar to the relationships between these parameters and remotely sensed spectral data from other studies. In particular, typical inverse curvilinear form of the relationship was present, with gradually decreasing sensitivity of the NIR band with the increase of volume and AGB. The NIR band showed very small changes once the volume and AGB exceeded ~300 $m^3\,ha^{-1}$ and ~150 $t\,ha^{-1}$, respectively. The negative form of the relationship is typical for coniferous forests [4, 6]. This pattern is connected with the natural development of forest structure. With the aging of the forest, the number and size of gaps in the canopy increase [34]. The understory or the shorter trees filling the gaps are shaded by the adjacent higher trees. The structural complexity and increased shadowing in the older (and usually higher-volume/AGB) stands leads to an overall reduction of reflectance from the canopy [32, 35]. The reduction is observed even in the NIR range [37], despite the high NIR reflectance at the single-needle level.

The observed maximal correlation of the volume and AGB with the NIR band is in contradiction with the results of Muukkonen and Heiskanen [4]. These authors found that the volume and AGB in forests with similar composition to the forests in this study are most strongly correlated with the green band of the Advanced Spaceborne Thermal Emission and Reflection Radiometer (ASTER) satellite sensor. It can be speculated that this difference is due to the non-equal width of the spectral bands in SPOT 5 and ASTER or due to the fact that Muukkonen and Heiskanen [4] used atmospherically corrected image, whereas in this study, the atmospheric effects were not corrected. However, the maximal correlation of volume/AGB with the NIR band is not unusual and has been observed in previous studies, including those using SPOT data [6].

The vegetation indices that use the SWIR band did not provide for straightening the relationships in comparison with the NDVI, SR, and the spectral bands, which was unexpected. In fact, the SWIR band alone outperformed the NDII, SI, NDVIc, and RSR. As a rule the SWIR correction factor in NDVIc and RSR accounts for the canopy closer. This has been shown to improve the relationship with leaf area index (LAI) in open canopies by reducing the effect of background reflectance [28, 30]. In our study area, high canopy closure prevails, and background reflectance has minor importance, which can explain the failure of NDVIc and RSR to improve the relationship between satellite data and forest parameters.

Figure 7 shows that the general form of the relationship between the NIR band and the Volume/AGB is the same for both ground datasets -stands and plots. However, the mean volume and AGB were higher in the field plot dataset, and in it, the high values were better represented. Also, it seems that at certain radiance, plots tend to have higher volume and AGB than stands. It would be appealing to explain this with scale dependant spectral response patterns, but this hypothesis was not examined in this study. Alternatively, an important role of the

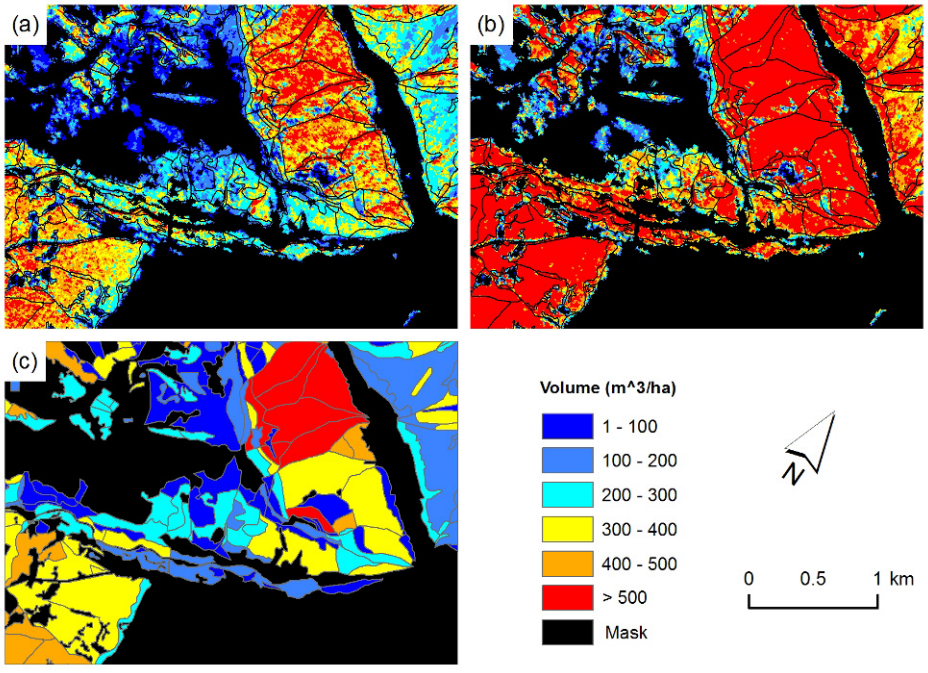

Figure 5. Fragments from maps of volume created by the NFI data (c) and by the regression models applied to the SPOT 5 NIR band (a and b). The models based on stand and plot data were used for (a) and (b), respectively. The borders from the NFI dataset were overlaid in (a) and (b) for better comparison.

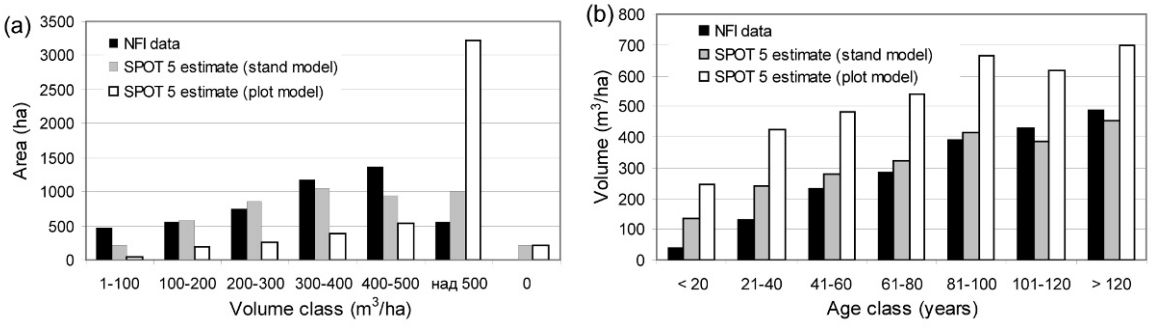

Figure 6. Comparison of the areas of volume classes (a) and the mean volume by age classes (b) according to NFI data and satellite-derived maps.

different methods of gathering ground data in the two datasets can be suggested. Gemmell [35] showed that the utility of TM data to estimate volume in mixed conifer species site was dependent on spatial scale. He found that sampling TM imagery in small areas (0.25 ha) was not suitable for specifying the relationship between TM data and the forest information and suggested that in small spatial areas, the sensitivity of measured radiance to stand characteristics like spatial gaps, variations in stand density, and background reflectance impeded estimation of volume [35]. However, in this study, sampling and modelling at plot level had better potential for volume

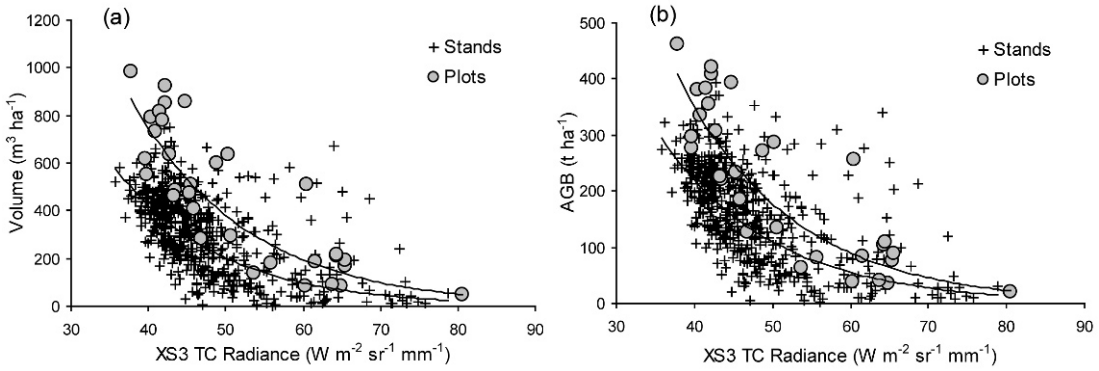

Figure 7. Scatterplots of topographically corrected NIR radiance from SPOT 5 against the volume (a) and AGB (b) from the two ground datasets. Smoothing trendlines were added for better comparison of plot and stand data.

and AGB prediction than the use of larger-area-averaged stand data as assessed by the R^2 and $RMSE_r$.

5.2. Topographic correction

Contrary to expectations, the topographic correction of the images did not improve the correlations between SPOT 5 data and volume and AGB. Similar results are reported by Turner *et al.* [36], who do not find apparent improvement in the fit for the LAI-SVI relationships as a result of the correction. Although positive effect of the SCS+C correction was not detected by the correlation coefficient, the use of topographically corrected images should be recommended. The reason for this is that topographic correction has no obvious harmful effect on the relationships, while at the same time, significantly reduces the hillshade pattern of the image. Without such a correction, the hillshade pattern would be transferred to the estimated volume or AGB raster surface.

5.3. Regression models

The accuracies of prediction of volume and AGB in this study were close to those reported in some previous studies of coniferous forests using similar type of data and methods (Table 7). The absolute errors ($RMSE$) in our study were highest of all authors cited in Table 7, but this could be expected since the forests studied here have higher volume and AGB, as indicated by their mean values. The RMSEr on the other hand, were relatively low, especially for the models generated by plot data. In the present study, the $RMSE_r$ for the volume was 33-45% depending on the type of used ground data, while in the discussed previous studies, the $RMSE_r$ varies from 32% to 67%. Almost the same values hold for the AGB (Table 7). Since the $RMSE_r$ is a measure of the relative importance of a certain amount of error with regard to the specific forest conditions, it is preferred in model comparisons. For example, while in a forest of low biomass, a $RMSE$ of 50 t ha^{-1} would likely be high, in a forest with biomass of 300 t ha^{-1} or so, this value would be far more acceptable. The present study showed that in the coniferous forests of the Rila Mountain, SPOT 5 data and regression approach can be used for volume and AGB prediction with the same success as in other coniferous forest types in Europe and North America, as concerned the $RMSE_r$.

Different factors, such as errors in ground data and georeferencing can contribute to the uncertainty of regression models. The errors in the NFI dataset are expected to be within 10-15%. The conversion coefficients for AGB are quite accurate, as reported by Zamolodchikov *et al.* [19] - the difference in the means between measurements and estimates using the coefficients being 1% for the Scots pine and 6% for the Norway spruce. However, it should be noted that these coefficients have been developed for different territory and may not be fully applicable over our study area. Errors in plot measurements may have been caused by the use of single value of q_2 for all trees within a species, regardless of their age. The determination of q_2 for every tree on the field was impossible. Errors in the biomass calculation in the plots may be also expected because of the use of mean values for the percent of foliage and branch biomass. In some places positional errors of up to several tens of meters were present in the stand borders data from the digitized paper map. As a result, some polygons may not be homogeneous, which changes the extracted reflectance characteristics, especially for the smaller stands [7]. In this

Table 7. Accuracy of volume and biomass predictions in coniferous forests according to some previous studies. Also shown are the mean values for the volume and biomass in the datasets used by the authors and the used satellite sensor.

Reference	Satellite sensor	Volume			Biomass		
		Mean	*RMSE*	$RMSE_r$	Mean	*RMSE*	$RMSE_r$
			($m^3 ha^{-1}$)	(%)		($t\,ha^{-1}$)	(%)
[5] [b]	–	187.0	–	58.0			
[5] [b]	Landsat *ETM+*	181.0	85.0	33.0			
[10] [b]	SPOT5 *HRG*	277.0	83.0	32.0			
[8] [b]	Landsat *TM*	135.8	71.3	47.6			
[7]	SPOT *XS*	156.5	78.9 [a]	50.0			
[37]	WorldView-2	61.5	27.2	44.2			
[4]	Terra *ASTER*	93.0	88.5	44.8	115.0	48.2	39.5
[38]	Landsat *ETM+*	194.1	70.0	36.1	114.4	37.6	32.9
[39] [b]	Landsat *TM*	182.0	–	66.6	92.3	–	66.5
[9]	Landsat *TM*				681.5	–	47.0 [a]
This study (stand model)	SPOT5 *HRG*	301.1	136.5	45.4	158.5	69.0	43.5
This study (plot model)	SPOT5 *HRG*	462.4	152.4	33.0	216.6	70.2	32.4

[a] the value shown is the standard error of estimate, not the RMSE

[b] kNN or other method was used by these authors, not the regression analysis.

study, these effects were partly removed by using only stands with area over one hectare and by masking the border pixels. A similar effect may be caused by logging a stand after the NFI have been carried out and before image acquisition. When such changes were identified on the image, the stand was removed from the analysis. However, not all changes may be visually recognized. Positional errors should have small effect on plot data, because of the generally good orthorectification results and the accurate GPS measurements.

The usefulness of the stand-level NFI data for regression modelling is an important issue in countries where this data are the only ground truth data available. In our case, the regression models for volume and AGB based on the NFI data had lower RMSE, but higher RMSEr compared to the regression models based on plot data. This discrepancy could be attributed to the statistical differences in ground data itself. Although they represent the forest in a same territory, the NFI data had lower value for the mean volume and AGB compared with the plot data (Table 7). Thus, the relative errors for the standwise models were 26-27% higher than for the plotwise models, even though the absolute errors were only 2 to 10% higher. The differences in the means of the two datasets hinder the comparison of model accuracies. One independent measure is how the model line fits the data. In our case, the R^2 were much higher for the models using plot data (Table 6). Another problem that further questions any comparisons is that the two ground datasets were created using different methodologies. This raises questions about the importance of the different sampling strategies and about the need for accuracy assessment of ground data. As shown in Figure 5 and Figure 6, the plotwise model strongly overestimates the volume as compared with the NFI data. It is not likely that this is an appropriate validation criterion, however, because the model was generated using different reference data. And finally, mismatch of the trendlines in Figure 7 should be attributed to real, scale-dependent physical processes or merely to errors in ground data. Unfortunately, we were unable to verify the accuracy of the data used in this study through independent means.

Each of the two types of ground data has its advantages. The using of existing NFI stand data allows using larger sample size, which is important for every statistical procedure, including regression. On the other hand, when ground data are gathered from specifically designed network of plots (for example as a part of a project activity), better sampling and accuracy control may be achieved and parameters not included in the NFI may be measured, if required. Also, the introduction of noise in the model caused by errors in the stand borders map and stand heterogeneity may be avoided when using plots.

5.4. Forest mapping and applicability

Good agreement between the NFI volume map and the map generated from SPOT 5 image and the stand model was observed (Figure 5a and Figure 4c). Most of the differences were not greater than one volume class. Moreover, part of the differences may be due to heterogeneity of the stands, which is not resolved in the NFI polygon data. One advantage of the satellite-derived map is the better representation of the coniferous forest extent. It was determined by unsupervised classification of the SPOT 5 image and all other territories were

masked. For example, many young stands occupying former pastures (the upper left part of the map fragments in Figure 5) do not exist in the NFI map, but were mapped using the satellite data.

The suitability of the proposed regression models varies with the specific application and its accuracy requirements. According to the current regulations in Bulgaria, the errors in forest inventory data used to support operational activities in forestry should not exceed 10-15%. Therefore, the models presented here can not be applied for this purpose. However, data about volume and AGB are needed not only for operational purposes, but also for planning and development of different strategies [40]. Fazakas *et al.* [39] show that RMSE decreases with the increase of the area of aggregation of the estimates obtained from satellite data and reaches acceptable level for areas over 100 ha. As the biases of the proposed regression models were not significant and the residuals were more or less random, the averaged models' estimates should be close to the actual mean values of volume and AGB in a territory. To test the possibilities for making more general assessments, we compared the growing stock for all the NFI dataset with the estimates of the standwise regression model for the same territory (486 ha). The growing stock according to the NFI data was 1.65 millions m^3, and according to the SPOT 5 derived map - 1.75 millions m^3. The relatively small difference (6.2%) between the two sources of data confirmed the potential for general assessments of timber resources.

6. Conclusions

The SPOT 5 satellite data combined with regression analysis showed good potential for volume and AGB mapping in the studied mountainous region of Bulgaria. The relative errors of the estimates were not higher than those reported in literature for other regions, and as regards to the models developed by data from the field plots, they were lower than in most previous studies. Although the absolute errors were high, the results are reasonable having in mind the characteristically high biomass of the studied forests - conditions under which estimation of forest parameters by satellite spectral data is usually difficult. Remote sensing estimation of volume and AGB can be of benefit for forest management and protection in the studied region by providing cost effective data suitable for preliminary planning, transitional data updating and monitoring, and ecological studies. For these applications arrangement of the estimates in broad classes may be sufficient. Another possibility is to use the obtained raster layers for estimating the mean values for a larger area, such as compartment or administrative forestry unit. The topographic correction of the SPOT 5 image using the SCS+C method provided good results as assessed by the visual inspection of the image. This technique should be advised when regression models are to be developed in areas with high relief. Without topographic correction unrealistic spatial distribution of the modelled volume/AGB is observed, with consistently higher values on weakly illuminated slopes. Further studies are needed in order to find if scale affects the strength of the modelled relationships and if any reasons exist to prefer either plotwise or standwise data. The current study pointed out the importance of the source and methodology behind the ground data used for regression modelling of forest parameters.

Acknowledgments

We would like to thank to ASTRIUM for providing the SPOT image used in the study free of charge as part of a project under the Planet Action initiative. ASTER GDEM v.2 is a product of METI and NASA and is provided free of charge to the public. The field work was partly funded by the European Social Fund through contract with the Ministry of Education of Bulgaria (No. BG051PO001/07/3.3-02/63/170608). Special thanks to Kiril Dimitrov for the invaluable help during the field studies. We express gratitude to the reviewers of the manuscript for their constructive comments and suggestions.

References

[1] Dimitrov E., Modelirane na biomasata na estestvenia bial bor [Modeling of the biomass of the natural Scots pine], Pensoft, Sofia, 2001 (in Bulgarian)

[2] Berterretche M., Hudak A. T., Cohen W. B., Maiersperger T. K., Gower S. T., Dungan J., Comparison of regression and geostatistical methods for mapping Leaf Area Index (LAI) with Landsat ETM+ data over a boreal forest, *Remote Sens. Environ.*, 2005, 96, 49-61

[3] Cohen W. B., Maiersperger T. K., Gower S. T., Turner D. P., An improved strategy for regression of biophysical variables and Landsat ETM+ data, *Remote Sens. Environ.*, 2003, 84, 561-571

[4] Muukkonen P., Heiskanen J., Estimating biomass for boreal forests using ASTER satellite data combined with standwise forest inventory data, *Remote Sens. Environ.*, 2005, 99, 434-447

[5] Reese H., Nilsson M., Pahlén T .G., Hagner O., Joyce S., Tingelöf U., Egberth M., Olsson H., Countrywide Estimates of Forest Variables Using Satellite Data and Field Data from the National Forest Inventory., *Ambio*, 2003, 32, 542-548

[6] Ripple W., Wang S., Isaacson D., Paine D., A preliminary comparison of Landsat Thematic Mapper and SPOT-1 HRV multispectral data for estimating coniferous forest volume, *Int. J. Remote Sens.*, 1991, 12, 1971-1977

[7] Hyyppä J., Hyyppä H., Inkinen M., Engdahl M., Linko S., Zhu Y., Accuracy comparison of various remote sensing data sources in the retrieval of forest stand attributes, *Forest Ecol. Manag.*, 2000, 128, 109-120

[8] Mäkelä H., Pekkarinen A., Estimation of forest stand volumes by Landsat TM imagery and stand-level field-inventory data, *Forest Ecol. Manag.*, 2004, 196, 245-255

[9] Lefsky M. A., Cohen W. B., Spies T. A., An evaluation of alternate remote sensing products for forest inventory, monitoring, and mapping of Douglas-fir forests in western Oregon, *Can. J. Forest Res.*, 2001, 31, 78-87

[10] Wallerman J., Holmgren J., Estimating field-plot data of forest stands using airborne laser scanning and SPOT HRG data, *Remote Sens. Environ.*, 2007, 110, 501-508

[11] Leboeuf A., Beaudoin A., Fournier R. A., Guindon L., Luther J. E., Lambert M. C., A shadow fraction method for mapping biomass of northern boreal black spruce forests using QuickBird imagery, *Remote Sens. Environ.*, 2007, 110, 488-500

[12] Meyer P., Itten K., Kellenberger T., Sandmeier S., Sandmeier R., Radiometric corrections of topographically induced effects on Landsat TM data in an alpine environment, *ISPRS J. Photogramm.*, 1993, 48, 17-28

[13] Colby J., Keating P., Land cover classification using Landsat TM imagery in the tropical highlands: the influence of anisotropic reflectance, *Int. J. Remote Sens.*, 1998, 19, 1479-1500

[14] Vicente-Serrano S., Pérez-Cabello F., Lasanta T., Assessment of radiometric correction techniques in analyzing vegetation variability and change using time series of Landsat images, *Remote Sens. Environ.*, 2008, 112, 3916-3934

[15] Dorren L., Maier B., Seijmonsbergen A., Improved Landsat-based forest mapping in steep mountainous terrain using object-based classification, *Forest Ecol. Manag.*, 2003, 183, 31-46

[16] Petkov P., Penev N., Marinov M., Nedjalkov S., Naoumov Z., Garelkov D., Antonov G., Tipove gora I organizacia na gorskoto stopanstvo v tehnicheskia uchastak Govedartsi na Samokovskoto gorsko stopanstvo [Forest types and organization of forestry in Govedartsi technical area of the Samokov Forestry Enterprise], *Forest Science*, 1966, 3, 87-109 (in Bulgarian)

[17] Beruchashvili N., Zhuchkova V., Methods for complex physical-geographical investigations: The manual. Moscow University Press, Moscow, 1997 (in Russian)

[18] Dimitrov E., Gorskopromishlena taksatsia i lesoustroistvo [Forest mensuration and management]. University of Forestry Publishing House, Sofia, 2000 (in Bulgarian)

[19] Zamolodchikov D. G., Utkin A. I., Korovin G. N., Conversion coefficients phytomass/reserves related to dendrometric parameters and stand composition, *Forestry*, 2005, 6, 73-81 (in Russian with English summary)

[20] Land processes distributed active archive center (LP DAAC). Global Data Explorer. USGS, NASA. 2012. URL: http://gdex.cr.usgs.gov/gdex (last accessed 2012.10.24)

[21] Dimap dictionary-SPOT Scene profile Version 1.1.2. SPOT Image. 2006. URL: http://www.spotimage.com/dimap/spec/dictionary/dictionary.htm (last accessed 2012.01.22)

[22] Moran M. S., Jackson R. D., Slater P. N., Teillet P. M.,. Evaluation of simplified procedures for retrieval of land surface reflectance factors from satellite sensor output, *Remote Sens. Environ.*, 1992, 41, 169-184

[23] Kane V. R., Gillespie A. R., McGaughey R., Lutz J. A., Ceder K., Franklin J. F., Interpretation and topographic compensation of conifer canopy self-shadowing, *Remote Sens. Environ.*, 2008, 112, 3820-3832

[24] Teillet P. M., Guindon B., Goodenough D. G., On the slope-aspect correction of multispectral scanner data, *Can. J. Remote Sens.*, 1982, 8, 84-106

[25] Gu D., Gillespie A., Topographic normalization of Landsat TM images of forest based on subpixel Sun-canopy-sensor geometry, *Remote Sens. Environ.*, 1998, 64, 166-175

[26] Soenen S. A., Peddle D. R., Coburn C. A., SCS+C: a modified Sun-canopy-sensor topographic correction in forested terrain, *IEEE T. Geosci. Remote*, 2005, 43, 2148-2159

[27] Rouse J. W., Haas R. H., Schell J. A., Deering D. W., Monitoring vegetation systems in the Great Plains with ERTS. In: Freden S. C., Mercanti E. P., Becker M. A. (Eds.), Proceedings of the 3rd ERTS-1 Symposium, Vol.1, Sect. A, NASA, Washington, D.C., 1974, 309-317

[28] Nemani R., Pierce L., Running S., Band L., 1993. Forest ecosystem processes at the watershed scale: sensitivity to remotely-sensed Leaf Area Index estimates, *Int. J. Remote Sens.*, 1993, 14, 2519-2534
[29] Zheng D., Rademacher J., Chen J., Crow T., Bresee M., Moine J. Le, Ryu S., Estimating aboveground biomass using Landsat 7 ETM+ data across a managed landscape in northern Wisconsin, USA, *Remote Sens. Environ.*, 2004, 93, 402-411
[30] Brown L., Chen J. M., Leblanc S .G., Cihlar J., A Shortwave Infrared Modification to the Simple Ratio for LAI Retrieval in Boreal Forests: An Image and Model Analysis, *Remote Sens. Environ.*, 2000, 71, 16-25
[31] Hardisky M. A., Lemas V., Smart R. M., The influence of soil salinity, growth form, and leaf moisture on the spectral reflectance of Spartina alternifolia canopies, *Photogramm. Eng. Rem. S.*, 1983, 49, 77-83
[32] Gerylo G. R, Hall R.J, Franklin S. E, Gooderham S., Gallagher L. 2000. Modeling forest stand parameters from Landsat Thematic Mapper (TM) data. In: Proceedings of the 22nd Annual Canadian Remote Sensing Symposium, Victoria, British Columbia. 2000, 405-413
[33] Newman M. C., Regression analysis of log-transformed data: statistical bias and its correction, *Environ. Toxicol. Chem.*, 1993, 12, 1129-1133
[34] Spies T. A., Forest Structure: A Key to the Ecosystem, *Northwest Sci.*, 1998, 72, 34-39
[35] Gemmell F. M., Effects of forest cover, terrain, and scale on timber volume estimation with Thematic Mapper data in a Rocky Mountain Site, *Remote Sens. Environ.*, 1995, 51, 291-305
[36] Turner D. P., Cohen W. B., Kennedy R. E., Fassnacht K. S., Briggs J.M., Relationships between leaf area index and Landsat TM spectral vegetation indices across three temperate zone sites, *Remote Sens. Environ.*, 1999, 70, 52-68
[37] Ozdemir I., Karnieli A., Predicting forest structural parameters using the image texture derived from WorldView-2 multispectral imagery in a dryland forest, Israel, *Int. J. Appl. Earth Obs.*, 2011, 13, 701-710
[38] Hall R. J., Skakun R. S., Arsenault E. J., Case B. S., Modeling forest stand structure attributes using Landsat ETM+ data: Application to mapping of aboveground biomass and stand volume, *Forest Ecol. Manag.*, 2006, 225, 378-390
[39] Fazakas Z., Nilsson M., Olsson H., Regional forest biomass and wood volume estimation using satellite data and ancillary data, *Agr. Forest Meteorol.*, 1999, 98-99, 417-425
[40] Franklin S. E., Remote sensing for sustainable forest management, Lewis Publishers, Boca Raton-London-New York-Washington, 2001